Severe Weather

ANALYSIS OF SEVERE CONVECTION AND MERGING STORMS ON 22 JUNE 1984 WITH CONVENTIONAL AND DOPPLER RADAR

by Ron W. Przybylinski (1)
National Weather Service Forecast Office
Indianapolis, Indiana 46251
John E. Wright, Jr. (2)
National Weather Service Office
Evansville, Indiana 47711

ABSTRACT

An analysis is presented of severe convection that produced widespread damage over parts of northeast and east central Illinois and extreme west central Indiana during the afternoon and evening hours of 22 June 1984. Conventional radar reflectivity data from three locations displayed a persistent supercell exhibiting well known reflectivity characteristics. Two F1 scale tornadoes and one F0 scale tornado and extensive hailfall occurred during the storm system's lifespan. Marseilles's Doppler radar showed a persistent mesocyclone; however, tornadogenesis was not concurrently observed during mesocyclone recognition. The tornadoes formed during time periods when Doppler data for storm analysis was not available. During the later stages of the storm system's evolution, the supercell storm appeared to merge with another convective storm to form a second supercell. This supercell eventually produced the Hoopeston, Illinois tornado.

1. INTRODUCTION

During the afternoon and evening hours of 22 June 1984 several convective storms occurred over parts of northeast and east central Illinois and extreme west central Indiana. The intense storms persisted for nine hours and were observed by three radars over significant periods of their lifetimes. Two F1-scale tornadoes and one F0-scale tornado (3), minor wind damage, and copious amounts of hail were reported during the lifespan of these intense convective storms. No injuries occurred; however, property and crop damage was in the millions of dollars. Conventional radar reflectivity data from NWS (National Weather Service) radars at Marseilles, Indianapolis, and South Bend were utilized and presented in this study. Additionally, radial velocity data from the NWS Marseilles's Doppler sub-system are reviewed.

2. DATA

Low-level reflectivity data were obtained from the 10 cm WSR-74S (Weather Surveillance Radar) at Marseilles, Illinois and from the 5.4 cm WSR-74C systems at Indianapolis and South Bend, Indiana. The WSR-74S uses a common 3.7 m (12 ft.) diameter antenna with a 2.2 degree half-power beam width, while the WSR-74C uses a 2.4 m (8 ft.) diameter antenna with a 1.5 degree half-power beam width. Both radar observations (network and local) and 16 mm photographic film records of radar PPI (Plan Position Indicator) displays were used in this study. Radial velocities were observed on the EEC (Enterprise Electronics Corporation) Doppler sub-system at Marseilles with velocity data preserved on 35 mm photographic film.

3. SYNOPSIS

At 1800 GMT, the NMC surface analysis positioned a warm front from western Wisconsin to north central Illinois and central Indiana. Surface pressure gradients were weak over the region with surface high pressure centered on the East Coast. Low pressure over Kansas and Nebraska was advecting Gulf air into the Mississippi River Valley. Temperatures southwest of the warm front were in the 80's over Illinois and Missouri and dewpoints were in the 70's. Northeast of the front temperatures and dewpoints were both in the 60's.

Moderate warm advection over the area was apparent in the 1200 GMT 850 mb analysis. Simultaneously, a southeastward moving vorticity maximum at mid-levels, was over western Wisconsin. Low-level warm advection, PVA at mid-levels, and upper atmospheric diffluence combined to produce upward vertical motion over most of the upper Midwest.

A hodograph exhibiting the wind profile at Peoria, Illinois (1200 GMT, 22 June 1984) is shown in Fig. 1. The trace of the vertical wind shear over the lowest 6 km is quite similar to the wind profile of the supercell storm (4), (5), where the environmental winds veered with height. Stability indices recorded at 1200 GMT 22 June 1984, and 0000 GMT 23 June 1984 quantify the degree of instability over this area. Values of the 1200 GMT lifted index and total totals for Peoria, Illinois were -4 and 49 respectively; however, the degree of instability steepened at 0000 GMT with values reaching -6 and 52 respectively.

4. RADAR REFLECTIVITY

Network radar observations of low-level reflectivity for the time period 1630 to 0230 GMT, even hours, are shown in Fig. 2a. Additionally, the odd hours, 1730 to 0130 GMT are shown in Fig. 2b. Legibility of the diagrams was improved by reducing contour overlapping and elimination of less significant echoes. VIP (Video Integrator Processor) Levels 1, 2, and 3 are contoured and maximum

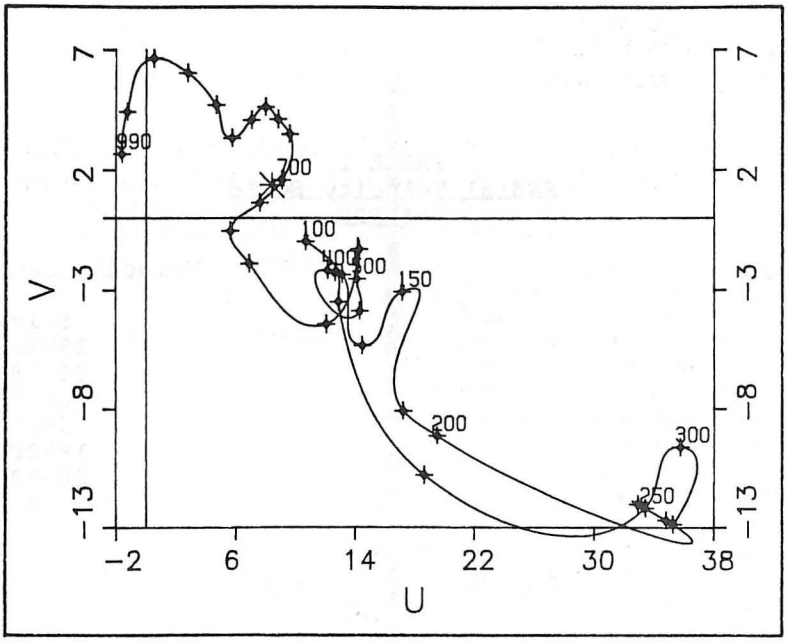

Fig. 1. Hodograph from Peoria, Illinois rawinsonde data at 1200 GMT, 22 June 1984. Wind speed is given in m s^{-1}.

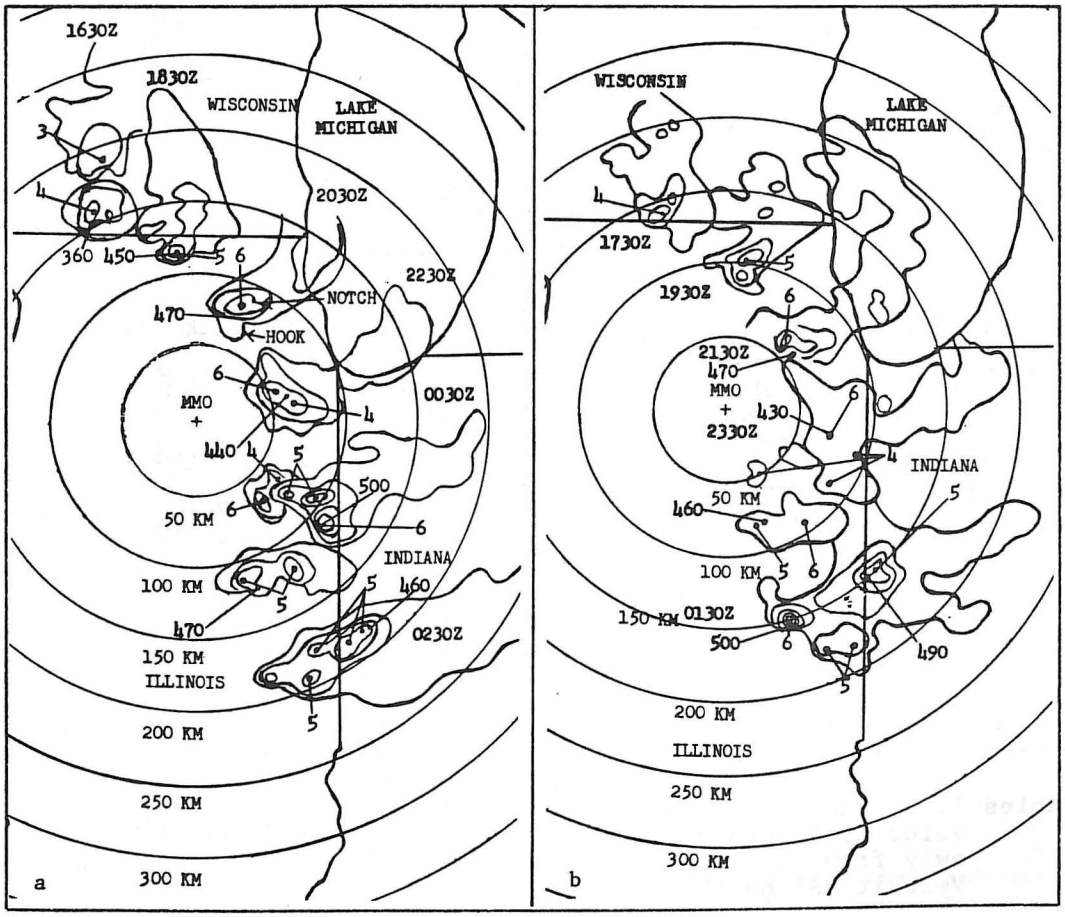

Fig. 2. Time sequence (GMT) of radar reflectivity data during the 22 June 1984 severe weather event. Reflectivity scans conducted at 0.5 degree elevation angle from the WSR-74S radar Marseilles, Illinois. VIP levels are contoured and maximum intensities labeled.

TABLE 1
Radial Velocity Scale
764 PRF

Direction	Velocity Range (mph)
T1,2	5-19
T3	19-28
T4	28-38
T5	38-47
A1,2	5-19
A3	19-28
A4	28-38
A5	38-47

TABLE 2
Radial Velocity Scale
917 PRF

Direction	Velocity Range (mph)
T1,2	5-22
T3	22-33
T4	33-44
T5	44-55
A1,2	5-22
A3	22-33
A4	33-44
A5	44-55

TABLE 3
Radial Velocity Scale
1100 PRF

Direction	Velocity Range (mph)
T1,2	5-26
T3	26-39
T4	39-52
T5	52-65
A1,2	5-26
A3	26-39
A4	39-52
A5	52-65

Tables 1, 2, and 3 - Radial Velocity Scales. "T" represents radial velocities toward the radar; "A" represents radial velocities away from the radar. Values less than 5 mph are shown as "Low Velocities" by the Doppler subsystem.

intensities indicated. Locations of most maximum echo tops with respect to low-level reflectivity are also shown. The approximate elevation angle was 0.5 degrees for all network radar observations.

Research of multicell and supercell storms has shown that a common pattern of evolution occurs in the storm structure. Lemon (6) used radar VIP in a PPI (Plan Position Indicator) tilt sequence mode to infer storm structure and develop severe weather warning techniques.

Lemon's derived criteria for a Severe Thunderstorm Warning are:

(1) VIP 5 echo at 8 km (27,000 ft. AGL) or higher.

In absence of (1), all the following must be satisfied:

(2) Peak mid-level, 4.9 to 11.9 km (16,000 to 39,000 ft. AGL), reflectivities must be equal to or greater than VIP 4.

(3) Mid-level echo overhang must extend at least 6 km beyond the outer edge of (or beyond the strongest reflectivity gradient of) the low-level echo.

(4) The highest echo top must be located on the storm flank possessing the overhang and be above the low-level reflectivity gradient between the echo core and echo edge or lie above the overhang itself.

Radar indication of a tornado requires the above 2, 3, and 4 criteria be satisfied and either or both:

(1) A low-level pendant (oriented generally at right angles to storm motion) exists, but may be embedded within lower reflectivities (the pendant must lie beneath or bound the overhang echo on the west).

(2) A BWER (Bounded Weak Echo Region) is detected.

Examination of the sequence of low-level reflectivities showed an area of thunderstorms over southern Wisconsin at 1630 GMT on 22 June 1984. Storm history included the occurrence of an F0 tornado at 1556 GMT, 70 km (38 nm) (nautical miles) northwest of JVL (Janesville, Wisconsin). Maximum echo tops were 11 km (36,000 ft.) with a VIP Level 4 approximately 50 km (27 nm) northwest of RFD (Rockford, Illinois). The maximum echo top was observed to be displaced over the sharpest low-level reflectivity gradient along the upwind flank (southwest quadrant) of the cell, but mid-level reflectivity data were missing (6). Apparently, a strong updraft was present with some low-level inflow. Cell movement was from 260 degrees at 10 m/s (20 kts).

By 1810 GMT the thunderstorms were organizing into a large severe storm located 20 km (11 nm) northwest of RFD. The maximum echo top had increased to 13.7 km (45,000 ft.) with a VIP 5 extending upward to 8.8 km (29,000 ft.). Such high reflectivities aloft are characteristics of hail shafts containing large hail (6). The maximum echo top was apparently over the low-level VIP 5 core - not a frequent characteristic of severe storms. However, the low-level reflectivity gradient had sharpened on the south flank of the cell.

The recent increases in VIP level, maximum echo top, and low-level reflectivity gradient apparently signified strong low-level inflow and updraft intensity as the storm was now moving from 290 degrees at 10 m/s (20 kts). Following severe storm development at 1830 GMT was tornadogenesis 28 km (15 nm) northeast of RFD, where an F1 tornado damaged a 119-year-old home, and severely damaged trees and power lines in the area.

During the time period 1830 to 2030 GMT, possible appendages and hook formations were visible on the southwest flank of the severe right moving storm. A sharp low-level reflectivity gradient persisted on the upwind flank (southwest quadrant) of the cell. Around 1900 GMT 4 cm (1 1/2 inch) diameter hail started to fall along the storm's southeast path. Additional observations of a large hail shaft in the cell occurred at 1930 GMT with a VIP Level 6 up to 12.2 km (40,000 ft.). Later, at the 2000 GMT, the maximum height of the VIP Level 6 descended by 3 km (10,000 ft.) to 9.1 km (30,000 ft.) with a maximum echo top of 14 km (46,000 ft.). The top was shifted over the low-level reflectivity gradient and mid-level echo overhang apparently exceeded 6 km. Descent of the VIP Level 6 storm core was followed by the observation of a possible hook echo at 2013 GMT on the southwest flank of the cell.

By 2030 GMT the maximum echo top was still displaced over a sharp low-level reflectivity gradient along the inflow flank (south quadrant) of the supercell and mid-level echo overhang was still 6 km, or more. A hook echo was apparent in the VIP Level 1 pattern on the south west flank of the storm. Therefore, Lemon's criteria for a Tornado Warning was met at this time. Also, a downwind notch in the VIP Level 3 was present, apparently induced by diversion of ambient environmental winds around the intense updraft. Copious amounts of 4 to 7 cm (1 1/2 to 2 3/4 inches) diameter hail were reported from 2030 to 2137 GMT along the storm's path. At 2045 GMT, accumulations of hail up to 30 cm (one foot) deep and 27 m/s (54 kts) winds occurred near St. Charles, Illinois. However, no public reports of funnels or tornadoes were received during the evolution of the hook echo.

Lemon's severe thunderstorm criteria were again met from 2045 to 2200 GMT. The sharp low-level reflectivity gradient persisted on the south flank of the storm. An appendage was still present on the southwest flank of the supercell at 2058 GMT. During this period VIP 5 and 6 equivalent reflectivity levels continued to be observed up to 9.1 km (30,000 ft.) in the supercell. The VIP 6 level tilted south with height, implying significant mid-level overhang. Additional reports of large hail

were received, while the maximum echo tops consistently exceeded 12.2 km (40,000 ft.).

5. RADAR OBSERVATIONS OF MERGING STORMS

During the period 2200 to 2300 GMT, rapid development of new convective cells occurred downwind from the predominant supercell over northeast and east-central Illinois. Radar echoes from Indianapolis radar at 2328 are presented in Fig. 3. The predominant supercell which produced significant hail and damaging winds is labeled (A) while the new convective cells are labeled B (Hoopeston, Illinois storm, C. and D.

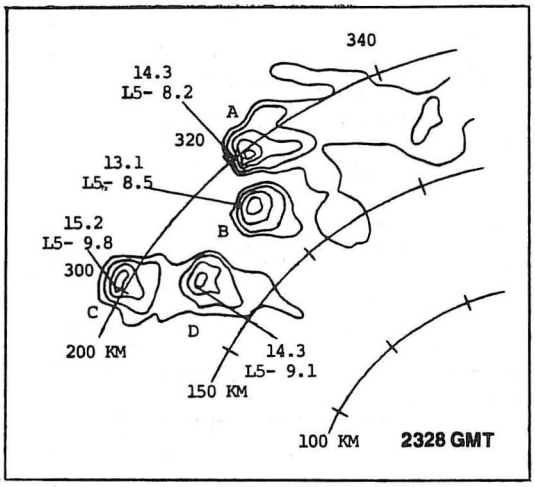

Fig. 3. Reflectivity scan at 0.5° elevation angle from the WSR-74C radar at Indianapolis, Indiana, at 2328 GMT on 22 June 1984. Reflectivity contours are 18, 30, 41, 50, and 57 dBZ respectively. Maximum echo height and height of VIP 5 (50 dBZ) are given in kilometers.

At 2328 GMT supercell characteristics continued to be observed with Convective Cell A. A sharp low-level reflectivity gradient persisted along the southern flank with the maximum echo top above it. Significant mid-level overhang exceeding 6 km was observed from Indianapolis radar. The maximum echo top of Convective Cell A reached 14.3 km (47,000 ft.) while its corresponding VIP 5 reflectivity core extended upward to 8.2 km (27,000 ft.). Convective Cells B, C, and D gradually developed severe storm characteristics after 2300 GMT with strong low-level reflectivity gradients and notches along the inflow side of each of these convective cells. The Hoopeston storm (Cell B), which developed directly south of the supercell (Cell A), had a maximum echo top of 13.1 km (43,000 ft.) with a VIP 5 core extending to 8.5 km (28,000 ft.). Convective Cells C and D were slightly more impressive with maximum echo tops exceeding 14.3 km (47,000 ft.) and VIP 5 reflectivity cores reaching 9.8 km (32,000 ft.) and 9.1 km (30,000 ft.) respectively. The strength of these two convective cells was probably a result of their proximity to high equivalent potential temperature 350° K air being advected from the south and southwest. Hail 2 to 5 cm (3/4 to 2 inches) in diameter was observed along the south and southwest flanks of each of the four convective cells as they moved across east-central Illinois.

A sequence of low-level PPI cross-sections between 2345 and 0051 GMT is shown in Fig. 4. Examination of the reflectivity data, showed a gradual merger between the supercell (Cell A) and the Hoopeston storm (Cell B). Examination of earlier radar reflectivity scans (2200 - 2300 GMT) revealed that the Hoopeston storm was significantly less intense than Cell A prior to merger between the two cells. During earlier scans, Cell A continued to exhibit supercell characteristics: intense low-level reflectivity gradients, well developed mid-level overhang, downwind "V" notch, displacement of maximum echo top and a right moving character by which we can infer that the storm had cyclonic rotation. As the supercell (Cell A) approached the Hoopeston storm (Cell B) significant changes in echo height and intensity occurred with both storms. During the period 2328 to 0003 GMT, the Hoopeston storm significantly intensified as its maximum echo top increased from 13.1 km (43,000 ft.) to 14.3 km (47,000 ft.) while its VIP 5 reflectivity core ascended from 8.5 km (28,000 ft.) to 10.4 km (34,000 ft.). On the other hand, Cell A lost its supercell characteristics and weakened as its maximum echo top descended from 14.3 km (47,000 ft.) to 12.2 km (40,000 ft.) and the top of its VIP 5 reflectivity core decreased from 8.2 km (27,000 ft.) to 5.5 km (20,000 ft.).

Detailed radar reflectivity scans from Indianapolis suggest that the two storms did not merge together in a dynamic sense. Rather we observed a continuous intensification of the Hoopeston storm (Cell B) and decline of the supercell (Cell A). It appears that the Hoopeston storm significantly disrupted the moist low-level inflow region of the supercell storm, which led to its detensification. Klemp et al (7) observed and studied a severe weather event in central Oklahoma where this process occurred between a storm having right moving characteristics and a significantly less intense convective cell.

During the period 0003 to 0100 GMT, Convective Cell A continued to further weaken while the Hoopeston storm intensified and evolved into a supercell. A sharp low-level reflectivity gradient developed along the southern flank of the Hoopeston storm, while notches and an appendage appeared on the southwest flank of the supercell (0021 GMT). Additional reflectivity characteristics, such as significant mid-level echo overhang exceeding 6 km and displacement of the maximum echo top over the inflow flank, further indicated that the Hoopeston storm had become a supercell. At this time the maximum echo top of the Hoopeston storm reached 13.7 km (45,000 ft.) while its VIP 5 reflectivity core maintained a maximum height of 10.4 km (34,000 ft.). Between 0020 and 0030 GMT the appendage gradually increased cyclonic curvature, while significant hail of 2 to 7 cm (3/4 to 2 3/4 inches) was reported. However, during this time no tornado was observed.

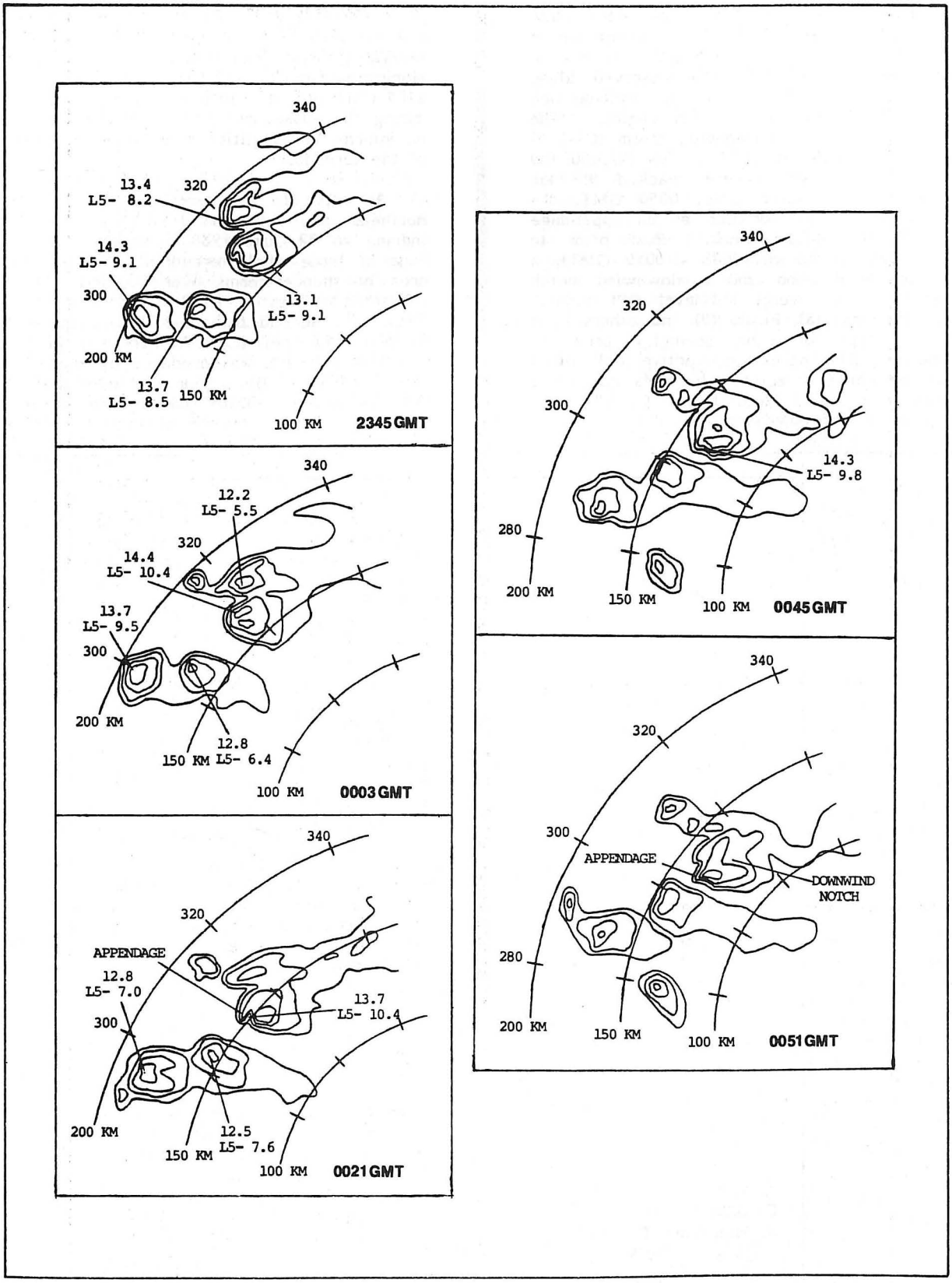

Fig. 4. Time sequence (GMT) of radar reflectivity data from WSR-74C at Indianapolis, Indiana, on 22 June 1984. Contoured VIP levels as in Fig. 3. Maximum echo height and height of VIP 5 (50 dBZ) are given in kilometers.

The Hoopeston storm slightly weakened in size after 0030 GMT; however, the storm reintensified fifteen minutes later. After 0045 GMT an intense low-level reflectivity gradient was observed along the surface inflow flank and a well-defined appendage had re-developed in this region. The maximum echo top of the Hoopeston storm (Cell B) increased 1.5 km (5,000 ft.) to 14.3 km (47,000 ft.) and its VIP 5 reflectivity core reached 9.3 km (32,000 ft.). Five minutes later, 0050 GMT, the Hoopeston storm became tornadic as an appendage emerged near the inflow flank. Just prior to reported tornado touchdown (0048 - 0050 GMT), a "v-shaped" low-level echo and a downwind notch were observed from several low-level PPI scans. Whiton and Hamilton (8), Fujita (9) and others have observed this type of echo geometry prior to tornadogenesis. The parent convective cell often deforms as the entire structure becomes influenced by the tornado cyclonic circulation. A "V" notch usually appears on the downwind side of the echo.

By 0055 GMT, a F1 scale tornado touched down and damaged four mobile homes, a grain elevator, several garages, and snapped numerous power lines along a one mile path. The appendage dissipated by 0105 GMT and the Hoopeston storm slowly weakened during the subsequent twenty minutes. Fortunately, no injuries or fatalities occurred during the lifespan of the tornado.

A map of the severe weather events over northeast and east-central Illinois, and west-central Indiana on 22 June 1984 is shown in Fig. 5. The first of three small tornadoes was produced by the area of thunderstorms over southern Wisconsin, an F0 tornado located 70 km (38 nm) northwest of JVL. The second tornado, F1, was spawned by the incipient supercell (Cell A) northeast of RFD. The third tornado, F1, was produced by another supercell storm (Cell B) near Hoopeston, Illinolis. Additionally, a lengthy hail swath stretched from east of RFD to just north of Hoopeston. This swath

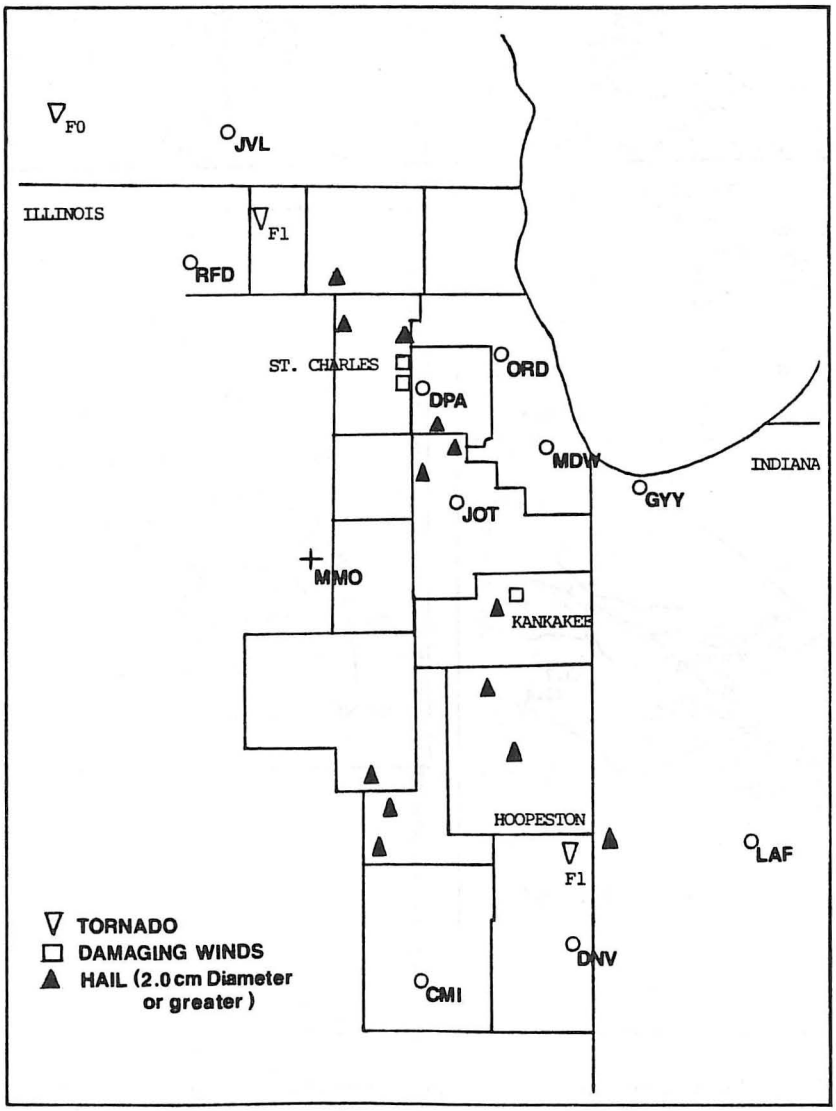

Fig. 5. Map of storm damage reports of the 22 June 1984 severe weather outbreak. Each report identified by ▽ tornado, □ damaging wind, or ▲ hail (2.0 cm diameter or greater).

was produced by a combination of the two southeastward moving supercells. Also, hail was deposited north of CMI (Champaign, Illinois) by the severe convective storm (Cell C) which developed downwind of the supercells.

6. RADIAL VELOCITY

In Figs. 6a - 6h a sequence of radial velocity patterns for the time period 1900 to 2138 GMT on 22 June 1984 are shown. Doppler radial velocities shown are the combination of motions within the storm system and the environmental winds. Dashed lines contour radial velocities directed toward the radar, while solid lines contour radial velocities directed away from the radar.

The Marseilles's Doppler can be operated at three PRF's (Pulse Repetition Frequencies): 764, 917, and 1100. While a higher PRF limits the range of the radar, it increases the threshold value of radial velocity at which "folding" occurs [velocity folding is a systematic misrepresentation of velocities which with experience can be properly interpreted by a trained observer (10)]. Velocity folding problems were periodically minimized by operation of the Doppler at higher PRF's. The radial velocity scales for 764, 917, and 1100 PRF's

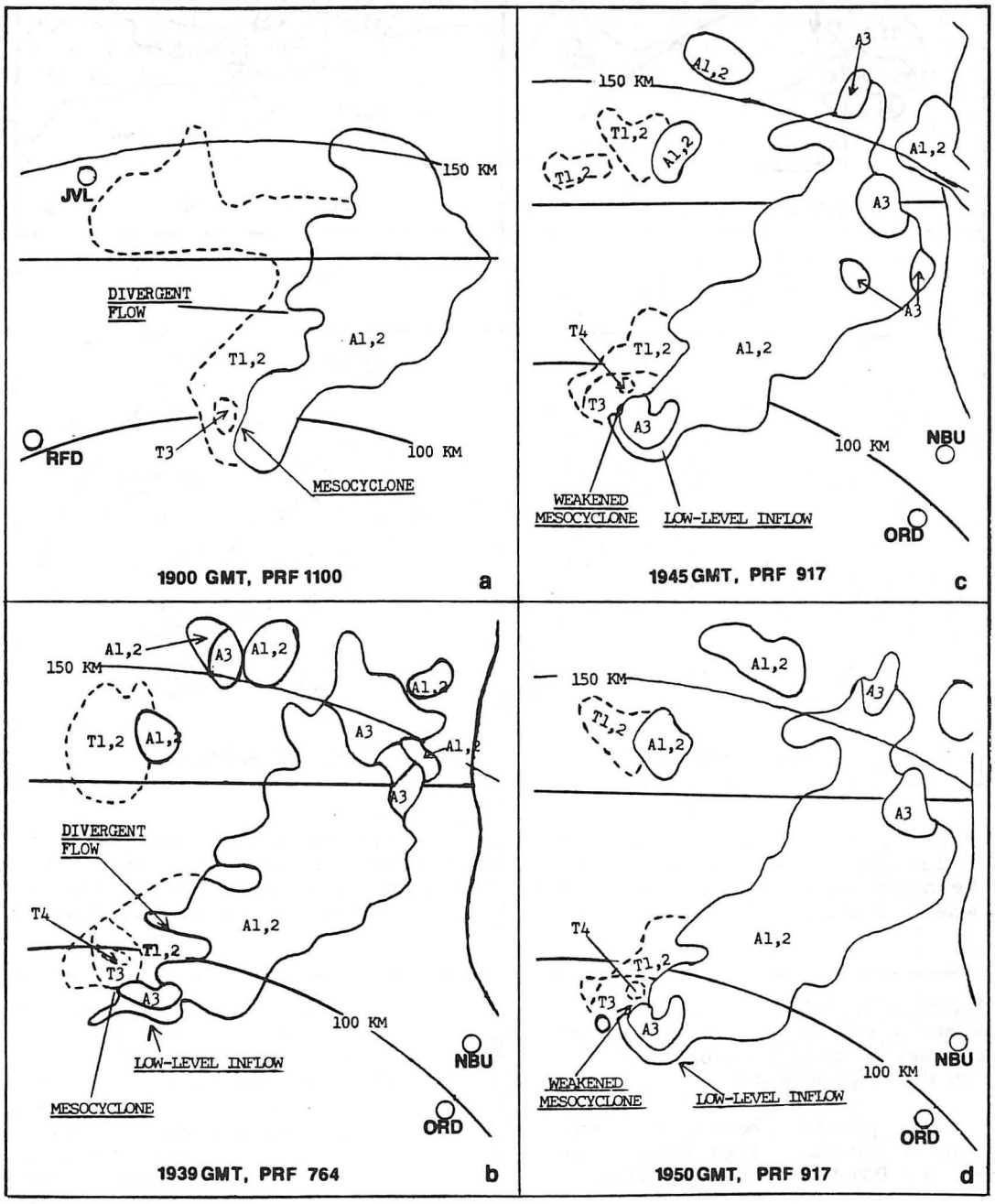

Fig. 6. Time sequence of Doppler velocity data from Marseilles, Illinois radar during the 22 June 1984 severe weather event. Velocity scans were conducted at 0.5° elevation angle. PRF (Pulse Repetition Frequency).

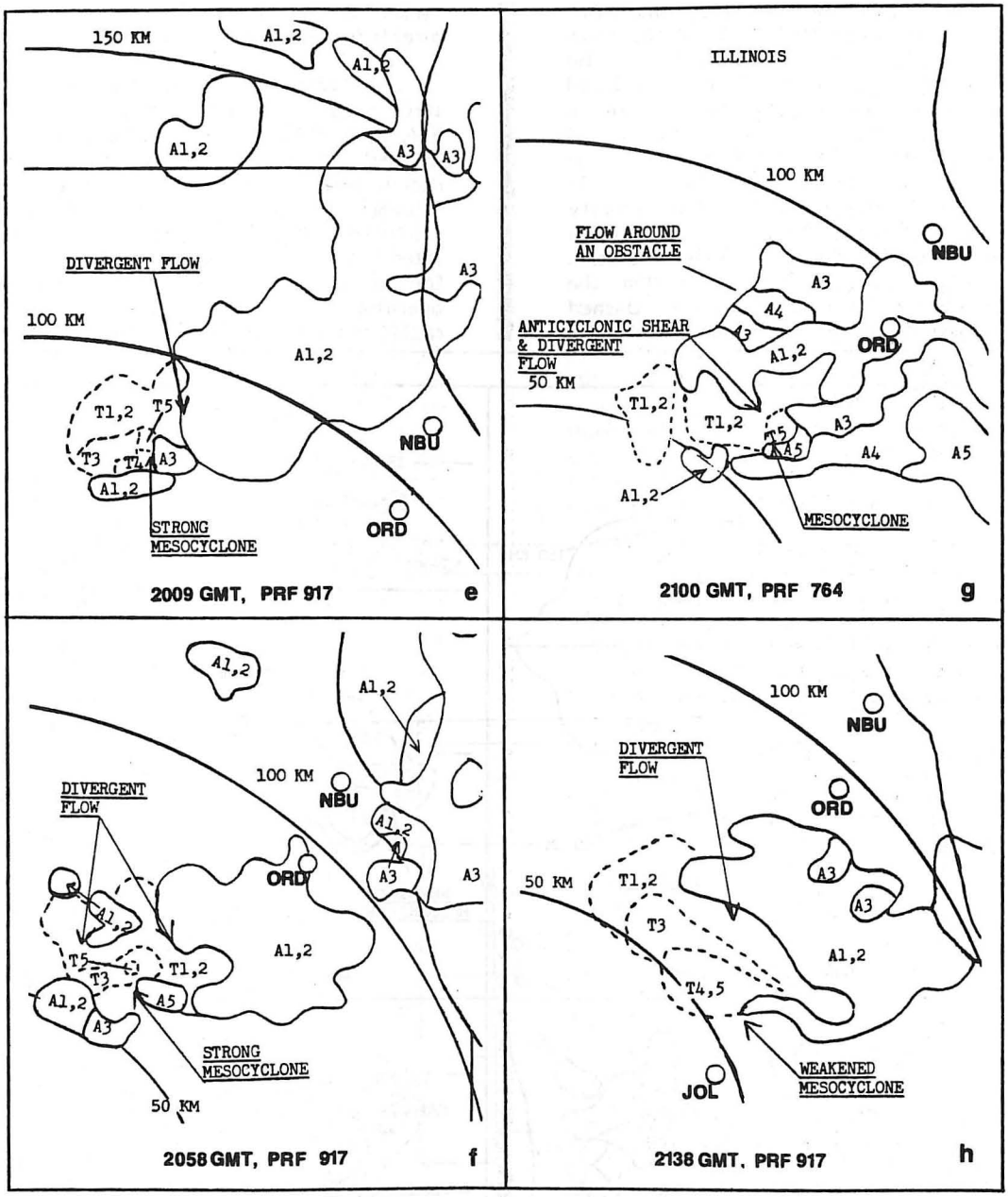

Fig. 6. Time sequence of Doppler velocity data from Marseilles, Illinois radar during the 22 June 1984 severe weather event. Velocity scans were conducted at 0.5° elevation angle except for (g) where elevation angle is 5.8°. PRF (Pulse Repetition Frequency).

are shown in Tables 1, 2, and 3. Each category in the tables represents a velocity with direction either toward (T) the radar, or away (A) from the radar; and speeds within the range indicated.

Donaldson (11) initially developed vortex signature recognition criteria. Then Burgess (12) refined and confirmed Donaldson's criteria. They are:

(1) Significant azimuthal shear (at least 5 x 10^{-3} s^{-1}) must exist between closed velocity contours (isodops) of opposite sign. The line between isodop centers must be skewed less than 45 degrees from a "constant-range" line.

(2) Shear pattern must extend vertically for a height interval comparable with the horizontal diameter. To be comparable the vertical extent can be as small as 50% of the horizontal diameter, but never can the vertical extent be less than 3 km (9,840 ft.).

(3) Shear pattern and closed isodops should persist for half the period required for

vortex revolution. For a single elevation angle the time period should be at least ten minutes.

(4) Shear pattern and closed isodops should remain invariant (constant) during a significant change in viewing angle (45 degrees or greater). This criteria has since been omitted by Burgess.

Examination of the 22 June 1984 storm system shows that a relatively large mesocyclone was apparently located in a supercell (Cell A), but the three criteria above were not consistently met. In Fig. 6a the radial velocities for 22 June 1984 at 1900 GMT are shown. PRF was 1100 and the center of the radar beam at the range of 100 - 120 km (54 - 64 nm) was about 1.8 km (6,000 ft.) above the surface. Examination of the data reveals some mesoscale flows characteristic of supercells. The authors believe a mesocyclone was present in the southwest quadrant of the storm. At this location cyclonic convergent rotation is visible as a T3/A1,2 couplet. This single Doppler velocity signature was modeled by Wood and Brown (13). While Burgess's (12) requirement of azimuthal shear equal to, or greater than 5×10^{-3} s^{-1} was not met, the line between isodops was skewed less than 45 degrees from a "constant-range" line. Observed estimates of azimuthal shear up to 4.2×10^{-3} s^{-1} were present in the southwest flank of the storm. However, true azimuthal shear was probably under-estimated, since the circulation was located 100 km (54 nm) north of MMO (Marseilles, Illinois). Donaldson (11) showed that the estimation of the actual peak velocity should consider the ratio of antenna beamwidth to vortex size. When this ratio is in excess of 1.5 the observed peak velocity is below it standard deviation, thus it would be wise to recognize the probable unreliability of a determination of the true maximum velocity in this circumstance. At this range the radar beam is 4.0 km (2.5 nm) wide and underestimation of azimuthal shear is probable due to reduction of maximum velocities produced by beam averaging. Network radar responsibilities prevented frequent horizontal observations or observation of the vertical extent of the shear pattern. Therefore, Burgess's shear pattern criteria for vertical extent and persistence for at least half the period required for vortex revolution were not directly applied. However, an F1 tornado was reported 28 km (15 nm) northeast of RFD at 1830 GMT. Also present in the 1900 GMT analysis was a divergent area northeast of the mesocyclone just south of the Illinois/Wisconsin state line. It appears as a couplet of isodops, A1,2/T 1,2 with opposite signs. Doswell and Lemon (14) proposed a three-dimensional depiction of evolution of the up (down) drafts, mesocyclone and tornadogenesis in an evolving supercell. In the supercell depiction a divergent downdraft, forward flank downdraft, was positioned northeast of the mesocyclone at low-levels. The divergent area 1900 GMT analysis) appears to be associated with the forward flank downdraft of the supercell.

A mesocyclone was still believed present at 1939 GMT in Fig. 6b, although Burgess's criteria for mesocyclone recognition were only partially met. An isodop couplet of opposite signs, T4/A3, was again present in the southwest quadrant of the supercell. The line between isodops was skewed less than 45 degrees from a "constant-range" line. Additionally, the shear pattern had existed long enough for the vortex to complete at least half a revolution. The average time required for half a revolution is six minutes (15).

Again, two assumptions were made. First, true azimuthal shear was greater than the indicated value of $3 - 4.2 \times 10^{-3}$ s^{-1} [the width of the radar beam, 4.4 km, (2.4 nm), at the range of the circulation, 90 km (49 nm) makes this assumption plausible]. Second, vertical extent criteria of the shear pattern were assumed met, due to the responsibility of network radar observations and limitations of the system. Figs. 6c and 6d show the radial velocity pattern for 1945 and 1950 GMT on 22 June 1984. The radial velocity patterns indicate a convergent mesocyclone signature modeled by Wood and Brown (13). While a T4/A3 couplet of isodops with opposite signs was present, the line between isodops had skewed more than 45 degrees from a "constant-range" line. The mesocyclone had apparently weakened considerably, since it no longer met the criteria for rotation. However, the authors believe a mesocyclone was still surviving on the southwest flank of the supercell since strong cyclonic shear remained (estimates of maximum azimuthal shear had increased to near 5.0×10^{-3} s^{-1}). Also, at this time 4 cm (1 1/2 inch) diameter hail was occurring with the storm.

By 2009 GMT the mesocyclone had strengthened. It is visible as a T5/A3 couplet of isodops with opposite signs in Fig. 6e, with an increased maximum azimuthal shear estimate of 7.7×10^{-3} s^{-1}. Secondly, the skewed angle was now less than 45 degrees from the "constant-range" line. Both values are indicative of a stronger rotational flow. Stronger and more concentrated generation of positive vorticity was occurring on the southwest flank of the storm. Therefore, a heightened probability of tornadogenesis was present, but not confirmed by reports. Again criteria for vertical extent of the mesocyclone were not applied.

Divergent flow northeast of the mesocyclone persisted to 2009 GMT but was less obvious in the velocity pattern. The divergent pattern was likely associated with the forward flank downdraft of the supercell.

The strong mesocyclone was still visible in the Doppler analysis for 2058 GMT Fig. 6f. It was present near the T5/A5 isodop interface. Estimates of maximum azimuthal shear had increased to 9.8×10^{-3} s^{-1}. Also, the skewed angle from the "constant-range" line remained less than 45 degrees. While the mesocyclone continued to be strong, no tornadogenesis was confirmed.

The significant areas of divergent flow are shown in the 2058 GMT analysis. The first area located northeast of the mesocyclone is associated with the forward flank downdraft. The second area located northwest of the mesocyclone was possibly associated with the rear flank downdraft (14).

Two minutes later at 2100 GMT in Fig. 6g the mesocyclone is visible at mid-levels 7.6 - 9.1 km (25,000 - 30,000 ft.), of the storm. A maximum azimuthal shear estimate of 8.4 x 10^{-3} s^{-1} was obtained at the T5/A5 isodop couplet. The velocity pattern was indicative of a dominant rotational flow on the southwest flank of the storm, but tornadogenesis still did not occur. Burgess's criteria for vertical extent of the shear pattern was met. Copious hail production was occurring as the mesocyclone flourished in the southwest quadrant of the supercell.

Another significant velocity pattern observed in the 2100 GMT analysis is similar to the enhanced-V detected in satellite imagery by McCann (16). A "flow around the obstacle" pattern appears as an area of low velocities, T1, 2, and A1, 2, flanked by higher away velocities. Both the enhanced-V and obstacle flow patterns are produced by similar kinematics and flowfields. Brown and Crawford (17) found that supercells act as quasi-solid cylinders impeding and diverting environmental winds around the updrafts. The environmental winds in the present case were estimated to be from 280 degrees at 15 - 20 m/s (30 - 40 kts) between the 500 to 300 mb levels. The component of environmental wind normal to the radar beam was lost, but evidence of an obstacle in the flow still appears in the observed component (Fig. 6g). Significant areas of anticyclonic shear are evident on the north side of the velocity pattern, while strong cyclonic shear and the mesocyclone are on the south side and areas of divergent flow are visible from northeast to northwest of the mesocyclone. Previously, on 27 April 1984 this pattern was observed at mid to upper-levels of the storm producing the Plainfield, Illinois tornadoes. Apparently, this velocity pattern is a good indicator of updraft strength and windshear at mid-levels of storm cells.

By 2138 GMT, Fig. 6h, the mesocyclone had weakened considerably. It is visible at the T4, 5/A1,2 interface on the southwest flank of the supercell. The maximum azimuthal shear value, 4.9 x 10^{-3} s^{-1}, had decreased and the skewed angle from the "constant-range" line was difficult to measure. Therefore, it appeared that rotational flow had decreased considerably and the threat of tornadogenesis had diminished. Also the area of divergent flow located north and northeast of the mesocyclone had expanded since 2058 GMT.

Further decay of the mesocyclone was evident from 2145 to 2200 GMT. After 2200 GMT the mesocyclone no longer appeared in the Doppler analysis. Radial velocity data were not obtained for the Hoopeston, Illinois storm.

7. CONCLUSIONS

Mesocyclone features of one supercell were observed with both conventional and Doppler radar over northeast Illinois. A second supercell was observed with conventional radar over east-central Illinois and extreme west central Indiana. Both supercells conformed to Lemon's severe thunderstorm and tornado detection criteria. However, Burgess's criteria for mesocyclone recognition were not consistently met during the history of the supercell.

The authors believe a mesocyclone was present on the southwest flank of one supercell (Cell A) from 1900 to 2200 GMT, but tornadogenesis was not reported. It is recommended that Burgess's first criteria be modified for Doppler data within 50 km (27 nm) to 100 km (54 nm), when the radar beamwidth is 2.0 degrees or more. Probability for mesocyclone detection for broad beam radars would be improved by the following:

1. Lowering the threshold value of azimuthal shear to 4.0 x 10^{-3} s^{-1}

The modification of mesocyclone criteria would compensate for averaging of velocities due to the radar antenna weighting function.

The authors are in agreement with recommendations from other Doppler research meteorologists who suggest that future Doppler surveillance radars possess a one degree or less beamwidth to improve beamwidth resolution.

Future observations of "flow around the obstacle" patterns in Doppler analysis should be regarded as indicators of intense convection. Also the strong areas of cyclonic shear on the south edge of the "flow around an obstacle" pattern should be watched for development of mesocyclones, or tornadic vortex signatures.

Both supercells satisfied Lemon's tornado detection criteria since the VIP 5 reflectivity core often exceeded 8 km (27,000 ft. AGL), a sharp low-level reflectivity gradient was noted along the inflow flank of the storm, and a pendant was observed near the southwest quadrant. Additional characteristics including significant mid-level echo overhang and the displacement of the maximum echo top over the inflow flank were also noted during the mature phase of each storm. The detection of the mesocyclone in Doppler radial velocity data further supported that the storm was potentially tornadic over northeast Illinois. However, no tornado was reported during the mesocyclone's lifespan over this region. The authors believe that no matter how strong the reflectivity characteristics and mesocyclone data are, there is always a small probability that tornadogenesis may not occur.

A decline of Cell A and the growth of Cell B (Hoopeston storm) was probably not due to a merger between the two storms in a dynamic sense. Rather, the probable disruption of the moist low-level inflow by the Hoopeston storm led to the weakening of the predominate supercell (Cell A).

ACKNOWLEDGEMENTS

The authors are especially grateful to Mr. Donald W. Burgess of the National Severe Storms Laboratory and Mr. Daryl L. Covey of the National Weather Service Training Center for their many beneficial suggestions for improving the manuscript. The authors would also like to express their gratitude to Dr. Joseph T. Schaefer (SSD CRH) of the National Weather Service for his encouragement and suggestions. Further, the authors acknowledge Mr. John T. Curran (MIC/AM) WSFO Indianapolis, and Mr. Norman Carroll (OIC) WSO Evansville for

their encouragement in this study. The authors would like to acknowledge Mr. Roy Wicinski (OIC) WSMO Marseilles for acquisition of radar reflectivity and Doppler velocity data and Mr. Larry Mowery (OIC) South Bend for the acquisition of radar reflectivity data.

NOTES AND REFERENCES

1. Ron W. Przybylinski is a Forecaster at the National Weather Service Forecast Office, Indianapolis. In addition to preparing aviation and public forecasts, he is also involved in severe storm meteorology, forecaster training and applied research.

2. John E. Wright, Jr. is Meteorologist and Radar Focal Point at the National Weather Service Office, Evansville. Previously, he was Meteorological Technician at the NWS Meteorological Observatory in Marseilles, Illinois. His interests include severe storm meteorology and applied research.

3. Fujita, T. T., 1981: Tornadoes and Downburst in the Context of Generalized Planetary Scales. J. Atm. Sci., 38, 1151-1534.

4. Davies-Jones, R. P., 1983: The Onset of Rotation in Thunderstorms. Preprints, Thirteenth Conf. on Severe Local Storms. Boston, Amer. Meteor. Soc. 215-218.

5. Weisman, M. L., 1984: Characteristics of Isolated Convection. AMS Intensive Course on Mesoscale Meteorology and Forecasting (Boulder). Amer. Meteor. Soc., Boston.

6. Lemon, L. R., 1980: Severe Thunderstorm Radar Identification Techniques and Warning Criteria. NOAA Tech. Memo. NWS NSSFC-3, 60 pp.

7. Klemp, J. B., P. S. Ray, and R. B. Wilhelmson, 1980: analysis of Merging Storms on 20 May 1977. Preprints, 19th Conf. on Radar Meteorology. Amer. Meteor. Soc., Boston, 317-324.

8. Whiton, R. C. and R. E. Hamilton, 1976: Radarscope Interpretation: Severe Thunderstorm and Tornadoes. AWS Tech. Rept. No. 76-266, 23 pp.

9. Fujita, T. T., 1973: Proposed Mechanism of Tornado Formation from Rotating Thunderstorms. Preprints, 8th Severe Local Storms Conf., Amer. Meteor. Soc., Boston, 191-196.

10. Covey, D. L., 1983: Doppler Weather Radar Principles. NOAA Training Paper, NWS TC-1, 19 pp.

11. Donaldson, R. J., 1970: Vortex Signature Recognition on a Doppler Radar. J. Appl. Meteor., 9, 661-670.

12. Burgess, D. W., 1976: Single Doppler Radar Vortex Recognition: Part I - Mesocyclone Signatures. Preprints, Seventeenth Conf. on Radar Meteor. Boston, Amer. Meteor. Soc., 97-103.

13. Brown, R. A. And V. T. Wood, 1983: Improved Severe Storm Warning Using Doppler Radar. Natl. Wea. Digest, 8, 17-27.

14. Doswell III, C. A. and L. R. Lemon, 1979: Severe Thunderstorm Evolution and Mesocyclone Structure as Related to Tornadogenesis. Mon. Wea. Rev., 107, 1184-1197.

15. Donaldson, R. J., 1986: Personal Communications, SASC Technologies, Inc., Lexington.

16. McCann, D. W., 1981: The Enhanced-Vee, A Satellite of Observable Severe Storm Signature, NOAA Tech. Memo, NSSFC-4, 31 pp.

17. Brown, R. A. and Crawford, K. C., 1972: Doppler Radar Evidence of Severe Storm High Reflectivity Cores Acting as Obstacles to Airflow. Proc. 15th Wea. Radar Conf., Amer. Meteor. Soc., Champaign-Urbana, 16-26.